How to cite: *Angew. Chem. Int. Ed.* **2023**, *62*, e202306183
doi.org/10.1002/anie.202306183

Zeolites

Dynamical Equilibrium between Brønsted and Lewis Sites in Zeolites: Framework-Associated Octahedral Aluminum

Mengting Jin, Manoj Ravi, Chen Lei, Christopher J. Heard, Federico Brivio, Zdeněk Tošner, Lukáš Grajciar, Jeroen A. van Bokhoven,* and Petr Nachtigall*[+]

Abstract: While the structures of Brønsted acid sites (BAS) in zeolites are well understood, those of Lewis acid sites (LAS) remain an active area of investigation. Under hydrated conditions, the reversible formation of framework-associated octahedral aluminum has been observed in zeolites in the acidic form. However, the structure and formation mechanisms are currently unknown. In this work, combined experimental ^{27}Al NMR spectroscopy and computational data reveal for the first time the details of the zeolite framework-associated octahedral aluminium. The octahedral LAS site becomes kinetically allowed and thermodynamically stable under wet conditions in the presence of multiple nearby BAS sites. The critical condition for the existence of such octahedral LAS appears to be the availability of three protons: at lower proton concentration, either by increasing the Si/Al or by ion-exchange to non-acidic form, the tetrahedral BAS becomes thermodynamically more stable. This work resolves the question about the nature and reversibility of framework-associated octahedral aluminium in zeolites.

Because aluminum in zeolites is responsible for the generation of both Brønsted-acid and Lewis-acid sites (BAS and LAS), which are responsible for catalytic activity, the state of aluminum in zeolites is the subject of many experimental and theoretical investigations.[1] The structure and properties of Brønsted acid sites in zeolite are well understood,[2] while those of Lewis acid sites in zeolites are not fully established. A zeolite BAS is associated with a bridging hydroxyl group between framework tetrahedrally coordinated aluminum and silicon atoms. Several types of LAS have been proposed,[3] including framework LAS,[4] extra-framework aluminum (EFAl)[5] and octahedral framework-associated aluminum.[6] The latter type, similar to the EFAl species, is typically characterized by an octahedral coordination of aluminum.[7] However, in contrast to EFAl species, the octahedral framework-associated aluminum can reversibly change its coordination between Al(T_d) and Al(O_h) (T_d: tetrahedral and O_h: octahedral).[6a] While the spectroscopic fingerprints of both Al(T_d) and Al(O_h) species are well known, the mechanism of the transition, the atomistic details of framework-associated Al(O_h), and the path of its conversion to a LAS site remain unclear. It is the goal of this investigation to combine biased ab initio molecular dynamics (AIMD) with ^{27}Al magic-angle spinning nuclear magnetic resonance (MAS NMR) spectroscopy on chabazite (CHA) zeolite towards understanding these details. CHA has been identified as an ideal zeolite for such investigation because it can be synthesized in wide range of Si/Al ratios, it has a suitable unit cell (UC) size for computational investigation, and it has a high symmetry structure with only a single crystallographically independent tetrahedral site and four independent framework oxygen positions. CHA consists of *cha* cages interconnected via 8R

[*] M. Jin, C. Lei, Dr. C. J. Heard, Dr. F. Brivio, Dr. Z. Tošner, Dr. L. Grajciar, Prof. P. Nachtigall[+]
Department of Physical and Macromolecular Chemistry, Charles University
Hlavova 8, 12843 Prague 2 (Czech Republic)
E-mail: lukas.grajciar@natur.cuni.cz

Dr. M. Ravi, Prof. J. A. van Bokhoven
Institute for Chemical and Bioengineering, Department of Chemistry and Applied Biosciences, ETH Zurich
8093 Zurich (Switzerland)
E-mail: Jeroen.vanbokhoven@chem.ethz.ch

Prof. J. A. van Bokhoven
Laboratory for Catalysis and Sustainable Chemistry, Paul Scherrer Institute
8092 Villigen (Switzerland)

M. Jin
Current address: Department of Physics, Yuxi Normal University
Yuxi 653100 (China)

Dr. M. Ravi
Current address: School of Chemical and Process Engineering, University of Leeds
Leeds LS2 9JT (UK)

Dr. F. Brivio
Current address: Department of Molecular Chemistry and Materials Science, Weizmann Institute of Science
Rehovot 76100 (Israel)

[+] deceased

window (3.8×3.8 Å).[8] Chabazite receives much interest, because Cu-CHA aluminosilicate and CHA-type SAPO-34 are the state-of-the-art catalysts for the selective catalytic reduction (SCR) of nitric oxides in vehicle applications and for the high performance in methanol-to-olefins conversion, respectively.[9]

Four samples of CHA have been considered in this work; their characteristics are shown in Table 1. Representative electron microscopy images are shown in Figure S1 in Supporting Information, accompanied by the energy-dispersive X-ray spectra (Figures S3, S4), which confirm that the vast majority (>90 %) of potassium cations have been ion-exchanged for ammonia cations. Thermogravimetric analysis of the H-CHA-450 (CHA in acidic form upon calcination at 450 °C) sample exposed to ambient conditions revealed 12 wt % of water, corresponding to an average concentration of 6 water molecules per CHA cavity (see Figure S2 in Supporting Information).

The ^{27}Al MAS NMR spectra presented in Figure 1 show that neither K-CHA nor NH_4-CHA showed any signal around 0 ppm corresponding to Al(O_h). On the contrary, calcination of NH_4-CHA leading to H-CHA-450 resulted in conversion of 22 % of Al(T_d) to Al(O_h), in addition to the formation of a broad shoulder, which monotonically decreases in amplitude from 50 to 10 ppm. Re-conversion of the sample back to NH_4-(H-CHA-450) by ion exchange with ammonium nitrate led to a significant reduction of the Al(O_h) signal around 0 ppm, while the broad shoulder remained mostly unaffected. We expect that the remaining Al(O_h) signal around 0 ppm after ion exchange is related to the EFAl species.[5] A constant Si/Al ratio (Table 1) indicates that no aluminum has been removed from the sample. Experimental data shows that that a significant fraction of Al(T_d) can reversibly transform to octahedral Al(O_h) and back, which is typical of acid zeolites.[6a,f]

The computational investigation was performed for a CHA model that mimicked the experimental conditions as closely as possible: unit cell with Si/Al=3 (the framework composition of $Si_9Al_3O_{12}H_3$) and six water molecules in the cavity (see above for experimental characteristics). Note that for topology reasons, there must be on average three Al atoms per double 6-membered ring (*d6r*) for CHA with Si/Al=3 and at least one Al–O–Si–O–Al pair. The particular configuration of Al atoms within the UC, and within *d6r*, is apparent from Figure S4 in Supporting Information; two Al atoms formed an Al–O–Si–O–Al pair while the third one was at least two $SiO_{4/2}$ units apart from other Al atoms. The computational protocol is based on recent studies of reversible hydrolysis of zeolite frameworks under aqueous conditions:[10] Biased ab initio molecular dynamics and thermodynamic integration were used for the calculations of the free-energy reaction paths connecting individual intermediates (see Section S2 in Supporting Information for details).

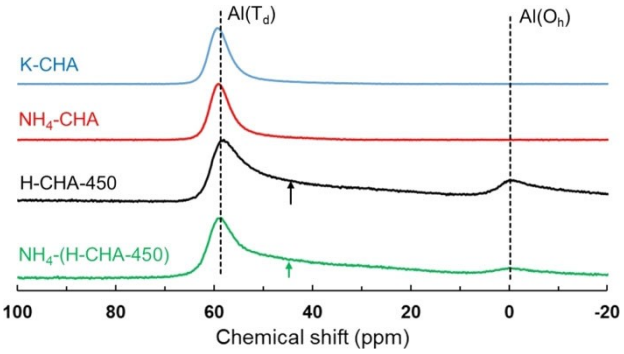

Figure 1. ^{27}Al NMR spectra of K-CHA, NH_4-CHA, H-CHA-450, and NH_4-(H-CHA-450). The arrow indicates the broadening of the peak associated with tetrahedral aluminum stretching towards lower chemical shifts.

The goal of our study was to identify and determine the structure and formation mechanism of the experimentally observed framework-associated Al(O_h). Starting from three BAS sites solvated by six water molecules, there is path towards a thermodynamically stable and kinetically allowed octahedral aluminum (Figure 2 and Table S2): Al is coordinated to three framework oxygens (O_f) and to three oxygens of water molecules (O_w) in the *fac*-Al(O_f)$_3$(H_2O)$_3$ arrangement (see Figure S4 for details). Thus, the octahedral aluminum is formally a coordinatively saturated Lewis acid site—it coordinates three water molecules—and it is denoted as LAS(6). Such framework-associated Al(O_h) is formed from one of the aluminum atoms constituting the Al–O–Si–O–Al pair: one of the Al–O–Si bonds in the six-ring is hydrolyzed, thus forming a silanol (Figure S4). None of the three original Brønsted protons in the CHA cavity are solvated upon the formation of Al(O_h): two of them are firmly attached to O_f atoms of Al(O_h) and the third one is consumed in the silanol formation (see below). Thus, the Al(T_d)→Al(O_h) conversion is associated with the loss of Brønsted acidity (three Brønsted protons are consumed). Analysis of the charge distribution shows +1.4 and −0.7 e charges on octahedral $AlO_{6/2}$ and tetrahedral $AlO_{4/2}$ species, respectively (see Section S3 in Supporting Information for details).

Table 1: Experimental characteristics of CHA samples.

Sample	Synthesis description	Bulk Si/Al	% Al(O_h)
K-CHA	Hydrothermal synthesis starting from zeolite Y	3.0	0
NH_4-CHA	NH_4^+ ion exchange of K-CHA	n.d.	0
H-CHA-450	Calcination in air at 450 °C Exposed to ambient conditions	3.0	22
NH_4-(H-CHA-450)	NH_4^+ ion exchange of calcined H-form	3.0	8

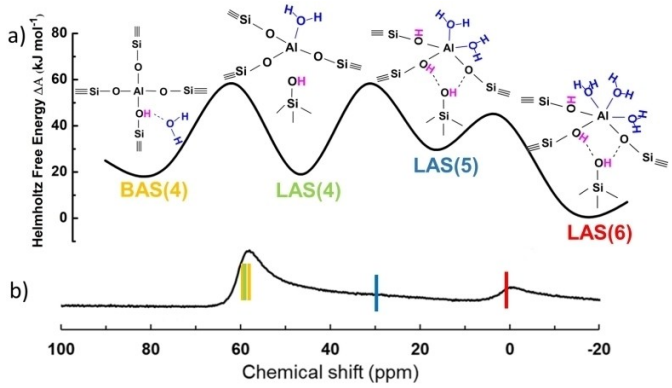

Figure 2. Structural, thermodynamic and NMR characteristics of tetrahedral and octahedral aluminum in zeolites. a) Schematic free energy profile connecting Brønsted acid site (BAS) with Lewis acid LAS(*n*) sites, *n* denotes the number of oxygen atoms in the first coordination shell of aluminium. b) Calculated chemical shifts for individual framework Al atoms compared with experimental data obtained for the same composition of the system (Si/Al = 3 and 6 water molecules per CHA cage). Colour code is for identification of BAS(4) and LAS(*n*) structures in the ^{27}Al NMR spectra.

While these structural characteristics are in line with the experimental insight, it is essential to understand both thermodynamics and kinetics of the Al(T_d)→Al(O_h) transformation. The transformation proceeds in three steps with each of four minima on the free-energy surface having a distinct aluminum environment (Figures 2a and S3, as well as cif files provided in Supporting Information). The initial CHA structure is taken as a reference state of the zeolite, in which all aluminum atoms are four-coordinated to framework oxygen atoms in T_d environment and six water molecules are in the cage. This reference is denoted BAS(4) in Figure 2a. The transformation towards octahedral LAS(6) starts with the formation of the Lewis acid site LAS(4) that is almost isoenergetic with BAS(4) and the transition is characterized by a moderate barrier of $\Delta A \approx 40\,kJ\,mol^{-1}$. The Al atom remains in a T_d environment and is coordinated to three O_f atoms and one water molecule. In the next step, two of the three framework oxygen atoms of the Al tetrahedron become protonated (accepting previously solvated protons, Figure 2a) and the second water molecule is bound to Al, forming a penta-coordinated LAS(5) structure; the free energy barrier is again around $40\,kJ\,mol^{-1}$ and the LAS(5) structure is slightly less stable than LAS(4). Transformation to octahedral aluminum is completed by accepting an additional water molecule to the first coordination shell of the Al atom. This is an exergonic process (by around $-30\,kJ\,mol^{-1}$) with a barrier as low as $15\,kJ\,mol^{-1}$. Under the simulation conditions (closely corresponding to the experimental situation) there are four stable local minima (Figure 2a), separated by modest free-energy barriers not exceeding $40\,kJ\,mol^{-1}$ that allow fast transitions between them, even at room temperature (RT).

Thermodynamically the most stable configuration is the octahedral LAS(6), which has a slightly lower free energy than the other intermediates. It is thus the most likely structure of one of the three Al atoms in the CHA unit cell (the other two Al atoms are not affected by the transformation and remain in T_d environments). We expect that the minor discrepancy between experimentally observed percentage of Al(O_h) in the H-CHA-450 sample (22 %) and the theoretical prediction (33 %) is mostly due to mildly inhomogeneous distribution of the aluminum and water in the experimental sample.

NMR chemical shifts for all these structures were calculated from time-averaged chemical shielding tensors and they are compared with experimental ^{27}Al NMR spectra in Figure 2b (see Section S2 in Supporting Information for details). A good agreement between experimental and calculated chemical shifts confirms the correspondence between experimentally observed and computationally found framework-associated Al(O_h). One possible explanation for the shoulder between 50 and 10 ppm is the presence of a significant proportion of LAS(5), which while thermodynamically unstable with respect to LAS(6), may persist for long timescales when there is a local deficit of water (one requires 3 available molecules to complete the transformation to LAS(6)). Another explanation is the previously reported asymmetric tetrahedrally coordinated aluminum species formed as a consequence of the irreversible thermal damage to the mordenite (MOR) framework (see section S4 in Supporting Information for more details).[6g] A third possibility, described in the Supporting Information (Figure S5) is broadening due to the incomplete solvation of protons on BAS(4) sites.

Both experimental evidence (investigation of samples with different Si/Al)[6d,e,11] and computational studies suggest that a critical local concentration of framework aluminum (and Brønsted sites) is required in order to form octahedral LAS(6). The roles of Si/Al, BAS site concentration, distance between framework Al atoms (all somewhat correlated) and the role of degree of hydration was therefore investigated next.

Experimental results show that the framework-associated Al(O_h) can be only detected for samples with sufficiently low Si/Al ratio and that this critical Si/Al ratio depends on the zeolite topology.[6d,12] The peak around 0 ppm, apparent only for the H-form of the zeolite and corresponding to framework-associated Al(O_h), is observed for CHA with Si/Al = 3 (Figure 1) while such a peak is not visible for H-CHA with higher Si/Al.[11] All attempts to localize a stable LAS(6), or any other octahedral Al structure, have failed for a CHA(Si/Al = 11) model containing just one Al atom in the *d6r*. Such structures spontaneously transform first to LAS(5) during the first few ps of an AIMD simulation and then further to LAS(4) after approximately 20 ps (Figure S11). Thus, LAS(4) and BAS(4) were the only kinetically stable structures found for CHA(Si/Al = 11) herein. In a previous study[10a] by some of us, we showed that BAS(4) and LAS(4) in CHA(11) are separated by a moderate barrier of $\Delta A^{\ddagger} < 40\,kJ\,mol^{-1}$, with both states characterized by similar free energies ($\Delta A_{rxn} \approx 20\,kJ\,mol^{-1}$ favoring BAS(4)).

Three protons are involved in the BAS(4)→LAS(6) transformation: two of them are firmly bound to Al-

(O_h)–O–Si bonds (Figure S6) while the third one forms a silanol group. This third proton contributes to the LAS(6) stabilization via H-bonding between the hydroxyl hydrogen and an Al(O_h)–O–Si oxygen atom that is not binding to a proton. We have attempted to determine how critical the presence of protons is on Al(O_h)–O–Si bridges (Figure 3a): Moving one of the protons from LAS(6) to one of the BAS(4) oxygens within the same CHA cage does not lead to the destruction of LAS(6). However, AIMD shows that the process is connected with an increase of system energy (+ 56 kJ mol^{-1}, Figure S8b). Moving both protons from LAS(6) to BAS(4) sites also leads to an increase of the system energy (≈20 kJ mol^{-1}, as is already seen from Figure 2a). However, this process involves a spontaneous transformation of LAS(6) back to LAS(4) and solvation of one of the protons, as shown in Figures 3b and S4c. Hence, the presence of at least one proton on an Al(O_h)–O–Si oxygen atom appears to be necessary for the localization of the octahedral Al moiety, and two are required to achieve stability.

One of the Al atoms of an Al–O–Si–O–Al pair transforms into LAS(6). A rather similar fac-Al(O_f)$_3$(H_2O)$_3$ complex was also found for the Al atom which is separated by at least two framework silicon from another framework aluminum and again, three protons were involved in the LAS(6) formation. However, this LAS(6) structure is less stable than the reference BAS(4) structure. The energy difference depends on the particular oxygen atom of the AlO_4 tetrahedron that is hydrolyzed in the first step of the reaction: energetic differences of +43, +29 and +91 kJ mol^{-1} were found for O4, O1 and O3 oxygens, respectively (Figure S9). This process cannot take place on O2 due to steric restrictions. Thus, the transformation from BAS(4) to LAS(6) is kinetically allowed even for Al atoms that are not involved in Al–O–Si–O–Al pairs. However, such a species is thermodynamically less stable and unlikely to be observed experimentally.

Individual water molecules are firmly bound to Al(O_h) as is shown in Figure 3c. Interaction energies for water molecules in the first (denoted 1, 2 and 3 in Figure 3c) and second (denoted 4–6) coordination shell are larger and smaller than −118 kJ mol^{-1}, respectively. The role of water quantity on the relative stability of LAS(6) and BAS(4) structures was investigated, by decreasing the number of water molecules in the CHA cage from six to three (removing all water from the second coordination shell). Very similar relative energies were obtained for LAS(6) and BAS(4) structures for both water concentrations. Thus, the stability of LAS(6) structure is not compromised even when the water loading is reduced to half (Figure S10).

To assess the generality of our findings, we also considered the formation of framework-associated Al(O_h) species in MOR models with Si/Al = 15 (containing one Al–O–Si–O–Al pair) and Si/Al = 47, with six water molecules in the unit cell (see section S2.1 for details). Similarly to the CHA case, our AIMD trajectories show that LAS(6) is kinetically stable only in the low-silica MOR model (Si/Al = 15) and that at least one proton bound to Al(O_h)–O–Si bonds appear to be necessary for the stabilization of the octahedral Al moiety (Figures S10, S11), while two protons

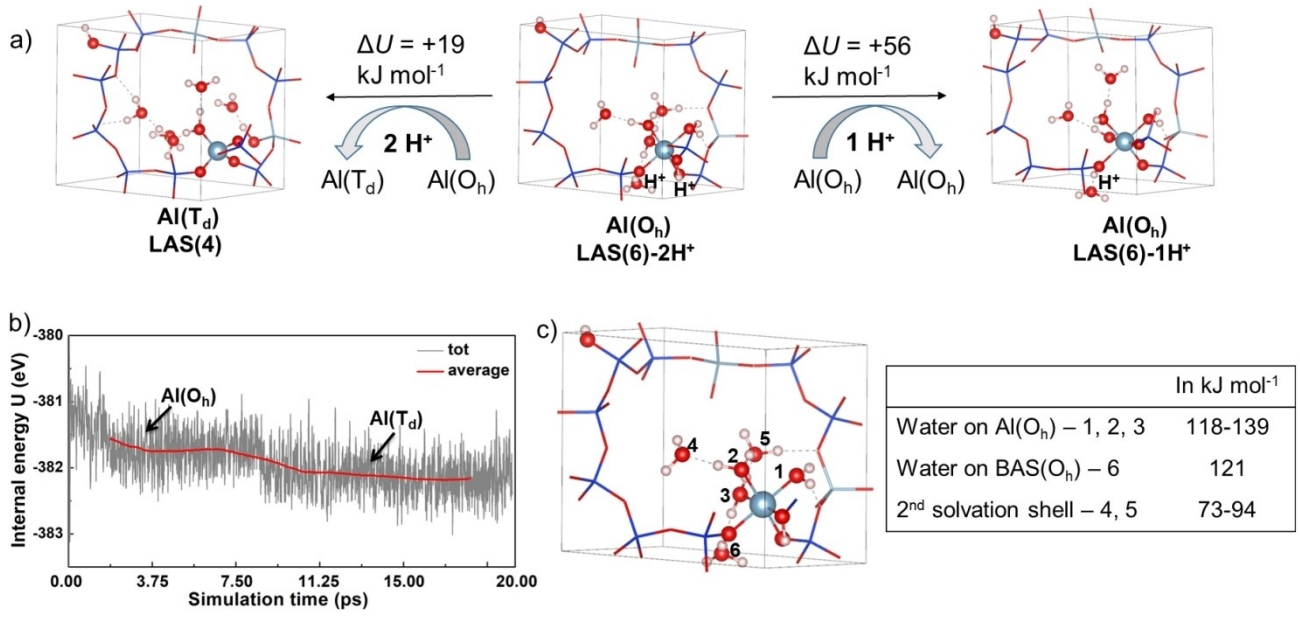

Figure 3. a) Structures and relative internal energies (at 300 K) of framework Al with different number of protons on the framework oxygen atoms of the first coordination shell of Al; Al(O_h) with two protons is thermodynamically the most stable (middle). The structure with one proton remains octahedral but is the least stable (right).The structure with no protons collapses to tetrahedral LAS(4) with a single water molecule attached to an Al atom (left). b) AIMD trajectory for octahedral LAS(6) with no protons evolving towards tetrahedral LAS(4) structure. c) Detachment energies of individual water molecules from the LAS(6) octahedral structure; 1st and 2nd coordination shell water molecules are numbered 1–3 and 4–6, respectively. Silicon atoms are in blue, aluminum in cyan, oxygen in red, and hydrogen in white.

stabilize the system further. These findings are in accord with previous experimental studies on MOR by some of us.[6e,g]

The results presented above show that thermodynamically stable and kinetically connected (to Brønsted acid sites at RT) framework-associated octahedral aluminum can be formed in CHA under the following conditions: (i) Three BAS sites must exist in close proximity to each other, to allow transfer and fixation of protons around the to-be-formed octahedral aluminum. (ii) Octahedral Al is formed from one of the Al atoms of the Al-pair, where Al atoms are separated by a single framework silicon atom. The former condition is, based on our calculations using MOR models (vide ante), likely to be general for zeolites and can be understood as arising from the large energetic penalty for the charge separation (Section S3 in Supporting Information), which increases with the increasing distance between three framework Al atoms involved in the LAS(6) formation. The latter condition, found to be valid both for CHA and MOR topologies, also appears to be generalizable, however, we expect that the effect of zeolite topology can be more pronounced than in the former case. This is highlighted by the recent observation that framework-associated octahedral aluminum species have a preferred location in the pore structure of MOR zeolite.[6g]

Our study brings additional evidence that the framework of acidic zeolites becomes labile under wet conditions[13] and the hydrolysis of zeolite Si–O–Al and Si–O–Si bonds is kinetically allowed at RT. This framework lability leads to a feasible, reversible transition between BAS and octahedral LAS(6), that is thermodynamically and kinetically feasible at RT and is governed primarily by proton concentration and aluminum density. Lastly, increased framework lability at low Si/Al ratios, at which Al-pairs are formed in CHA, may be one of the reasons for the quicker deactivation times in methanol-to-olefins conversion observed experimentally.[14]

Acknowledgements

Charles University Centre of Advanced Materials (CUCAM) (OP VVV Excellent Research Teams, project number CZ.02.1.01/0.0/0.0/15_003/0000417) is acknowledged. PN acknowledges the Czech Science Foundation (19-21534S) and LG acknowledges the support of the Primus Research Program of Charles University (PRIMUS/20/SCI/004) and that of Czech Science Foundation (23-07616S). Authors wish to thank to Vitaly L. Sushkevich for discussions and reading manuscript. Computational resources were provided by the e-INFRA CZ project (ID:90140), supported by the Ministry of Education, Youth and Sports of the Czech Republic. The authors would also like to acknowledge Dr. Frank Krumeich at ETH Zurich for support with electron microscopy analysis. J.A.v.B. and M.R. acknowledge ETH Zürich for financial support.

Conflict of Interest

The authors declare no conflict of interest.

Data Availability Statement

The data that support the findings of this study are openly available in Zenodo at https://doi.org/10.5281/zenodo.7794875.

Keywords: Ab Initio Molecular Dynamics · Octahedral Aluminum · Solid-State NMR · Zeolite Hydrolysis · Zeolites

[1] B. M. Weckhuysen, J. Yu, *Chem. Soc. Rev.* **2015**, *44*, 7022–7024.
[2] W. Haag, R. Lago, P. Weisz, *Nature* **1984**, *309*, 589–591.
[3] C. Chizallet, *ACS Catal.* **2020**, *10*, 5579–5601.
[4] a) K. Chen, Z. Gan, S. Horstmeier, J. L. White, *J. Am. Chem. Soc.* **2021**, *143*, 6669–6680; b) T. K. Phung, G. Busca, *Appl. Catal. A* **2015**, *504*, 151–157; c) S. Xin, Q. Wang, J. Xu, Y. Chu, P. Wang, N. Feng, G. Qi, J. Trebosc, O. Lafon, W. Fan, F. Deng, *Chem. Sci.* **2019**, *10*, 10159–10169; d) D. Coster, A. L. Blumenfeld, J. J. Fripiat, *J. Chem. Phys.* **1994**, *98*, 6201–6211; e) P. Y. Dapsens, C. Mondelli, J. Pérez-Ramírez, *ChemSusChem* **2013**, *6*, 831–839; f) G. L. Woolery, G. H. Kuehl, H. C. Timken, A. W. Chester, J. C. Vartuli, *Zeolites* **1997**, *19*, 288–296.
[5] a) U. Lohse, E. Löffler, M. Hunger, J. Stöckner, V. Patzelova, *Zeolites* **1987**, *7*, 11–13; b) S. M. T. Almutairi, B. Mezari, G. A. Filonenko, P. C. Magusin, M. S. Rigutto, E. A. Pidko, E. J. Hensen, *ChemCatChem* **2013**, *5*, 452–466; c) C. Liu, G. Li, E. J. M. Hensen, E. A. Pidko, *ACS Catal.* **2015**, *5*, 7024–7033; d) J. Holzinger, P. Beato, L. F. Lundegaard, J. Skibsted, *J. Phys. Chem. C* **2018**, *122*, 15595–15613; e) M. C. Silaghi, C. Chizallet, J. Sauer, P. Raybaud, *J. Catal.* **2016**, *339*, 242–255; f) X. Yi, K. Liu, W. Chen, J. Li, S. Xu, C. Li, Y. Xiao, H. Liu, X. Guo, S.-B. Liu, A. Zheng, *J. Am. Chem. Soc.* **2018**, *140*, 10764–10774.
[6] a) E. Bourgeat-Lami, P. Massiani, F. Di Renzo, P. Espiau, F. Fajula, T. Des Courières, *Appl. Catal.* **1991**, *72*, 139–152; b) A. Omegna, J. A. van Bokhoven, R. Prins, *J. Phys. Chem. B* **2003**, *107*, 8854–8860; c) J. A. van Bokhoven, H. Sambe, D. Ramaker, D. Koningsberger, *J. Phys. Chem. B* **1999**, *103*, 7557–7564; d) A. Abraham, S.-H. Lee, C.-H. Shin, S. B. Hong, R. Prins, J. A. van Bokhoven, *Phys. Chem. Chem. Phys.* **2004**, *6*, 3031–3036; e) M. Ravi, V. L. Sushkevich, J. A. van Bokhoven, *J. Phys. Chem. C* **2019**, *123*, 15139–15144; f) M. Ravi, V. L. Sushkevich, J. A. van Bokhoven, *Nat. Mater.* **2020**, *19*, 1047–1056; g) M. Ravi, V. L. Sushkevich, J. A. van Bokhoven, *Chem. Sci.* **2021**, *12*, 4094–4103.
[7] J. Jiao, J. Kanellopoulos, W. Wang, S. S. Ray, H. Foerster, D. Freude, M. Hunger, *Phys. Chem. Chem. Phys.* **2005**, *7*, 3221–3226.
[8] C. Baerlocher, L. B. McCusker, "Database of Zeolite Structures," http://www.iza-structure.org/databases.
[9] a) U. Olsbye, S. Svelle, K. Lillerud, Z. Wei, Y. Chen, J. Li, J. Wang, W. Fan, *Chem. Soc. Rev.* **2015**, *44*, 7155–7176; b) A. M. Beale, F. Gao, I. Lezcano-Gonzalez, C. H. F. Peden, J. Szanyi, *Chem. Soc. Rev.* **2015**, *44*, 7371–7405.
[10] a) C. J. Heard, L. Grajciar, C. M. Rice, S. M. Pugh, P. Nachtigall, S. E. Ashbrook, R. E. Morris, *Nat. Commun.* **2019**, *10*, 4690; b) M. Jin, O. Veselý, C. Heard, M. Kubů, P.

Nachtigal, J. Čejka, L. Grajciar, *J. Phys. Chem. C* **2021**, *125*, 23744–23757.
[11] J. R. Di Iorio, R. Gounder, *Chem. Mater.* **2016**, *28*, 2236–2247.
[12] A. Abraham, S. B. Hong, R. Prins, J. A. van Bokhoven, *Studies in Surface Science and Catalysis, Vol. 158* (Eds.: J. Čejka, N. Žilková, P. Nachtigall), Elsevier, Amsterdam, **2005**, pp. 679–686.
[13] a) C. J. Heard, L. Grajciar, P. Nachtigall, *Chem. Sci.* **2019**, *10*, 5705–5711; b) S. M. Pugh, P. A. Wright, D. J. Law, N. Thompson, S. E. Ashbrook, *J. Am. Chem. Soc.* **2020**, *142*, 900–906; c) C. J. Heard, L. Grajciar, F. Uhlík, M. Shamzhy, M. Opanasenko, J. Čejka, P. Nachtigall, *Adv. Mater.* **2020**, *32*, 2003264.
[14] M. A. Deimund, L. Harrison, J. D. Lunn, Y. Liu, A. Malek, R. Shayib, M. E. Davis, *ACS Catal.* **2016**, *6*, 542–550.

Manuscript received: May 3, 2023
Accepted manuscript online: June 7, 2023
Version of record online: June 7, 2023